Original Research

Involvement of cholesterol in synaptic vesicle swelling

Jin-Sook Lee, Won Jin Cho, Leah Shin and Bhanu P Jena

Department of Physiology, Wayne State University School of Medicine, Detroit, MI 48201, USA
Corresponding author: Bhanu P Jena, Department of Physiology, Wayne State University School of Medicine, 5245 Scott Hall, 540 E Canfield, Detroit, MI 48201, USA. Email: bjena@med.wayne.edu

Abstract

Studies demonstrate that cholesterol plays a critical role in the regulation of neurotransmitter release and that secretory vesicle swelling is a requirement for the regulated expulsion of intravesicular contents during cell secretion. In view of this, the involvement of cholesterol in synaptic vesicle swelling was hypothesized and tested in the present study, using isolated synaptic vesicles from rat brain and the determination of their swelling competency in the presence and absence of cholesterol. The involvement of the water channel aquaporin-6 (AQP-6) and proton pump vH^+-ATPase in GTP-$G_{\alpha o}$-mediated synaptic vesicle swelling has been reported previously. Mastoparan, the amphiphilic tetradecapeptide from wasp venom, known to activate the GTPase activity of $G_{\alpha o/i}$ proteins, stimulates synaptic vesicle swelling in the presence of GTP. In the current study, using nanometer-scale precision measurements of isolated synaptic vesicles, we report for the first time that depletion of cholesterol from synaptic vesicle membrane results in a significant loss of GTP-mastoparan-stimulable synaptic vesicle swelling. In contrast, incorporation of cholesterol into the synaptic vesicle membrane potentiates GTP-mastoparan-stimulable vesicle swelling. Our study further demonstrates that this effect of cholesterol is due, in part, to its involvement in the interactions between AQP-6, vH^+-ATPase and the GTP-binding $G_{\alpha o}$ protein at the synaptic vesicle membrane.

Keywords: synaptic vesicle, cholesterol, dynamic light scattering, photon correlation spectroscopy, atomic force microscopy

Experimental Biology and Medicine 2010; **235**: 470–477. DOI: 10.1258/ebm.2010.009259

Introduction

The fine-tuned composition of lipid and cholesterol in cellular membranes is known to play a crucial role in compartmentalizing various membrane proteins for specialized cellular activities.[1] Cholesterol has been proposed to play a critical role in regulating neurotransmitter release[2,3] and synaptic plasticity.[4] Vesicle volume increase following stimulation of cell secretion had previously been proposed as a result from studies using electrical measurements in mast cells[5–8] and in acinar cells of the exocrine pancreas.[9] However, the direct visualization of such an increase in secretory vesicle size at nanometer resolution in live cells following stimulation of secretion, and the central role of vesicle swelling in cell secretion, was first determined by Kelly *et al.*[10] Since then, our understanding of the molecular mechanism of secretory vesicle swelling has greatly advanced.[10–14] Isolated secretory vesicles and reconstituted swelling-competent proteoliposomes have been utilized previously[10–14] to determine the mechanism and regulation of secretory vesicle swelling. Isolated zymogen granules (ZGs), the secretory vesicles in exocrine pancreas, swell rapidly in response to GTP,[10–12] suggesting rapid water gating into them. Studies demonstrate the presence of the water channel aquaporin-1 (AQP-1) at the ZG membrane[11] and its participation in GTP-mediated water entry and vesicle swelling. Further, the molecular regulation of AQP-1 at the ZG membrane has also been examined,[9,11] providing a general molecular mechanism of secretory vesicle swelling. Immunoprecipitation of detergent-solubilized ZGs, using AQP-1 monoclonal antibody, co-isolates AQP-1, phospholipase A2 (PLA2), $G_{\alpha i3}$, potassium channel IRK-8 and the chloride channel ClC-2.[13] The exposure of ZGs to either the potassium channel blocker glyburide or the PLA2 inhibitor ONO-RS-082 blocks GTP-induced ZG swelling. Artificial liposomes reconstituted with the AQP-1-immunoisolated complex from solubilized ZGs also swell in response to GTP. Glyburide or ONO-RS-082 is found to abrogate the GTP effect in reconstituted liposomes. AQP-1 immunoisolate-reconstituted planar lipid membrane demonstrates conductance, which is sensitive to glyburide and an AQP-1-specific antibody. These results demonstrate a $G_{\alpha i3}$-PLA2-mediated pathway and potassium channel involvement in AQP-1 regulation at the ZG membrane,[13] contributing to ZG swelling. Similarly, AQP-6 involvement has

been demonstrated in GTP-induced and G_o-mediated synaptic vesicle (SV) swelling in neurons.[14]

In neurons, the water channel AQP-6 and the heterotrimeric GTP-binding protein $G_{\alpha o}$ at the SV membrane participate in rapid water gating and vesicle swelling.[14] Additionally, it has been shown that vH^+-ATPases are present at the SV membrane[15,16] and are responsible for the generation of electrochemical H^+ gradient (pH 5.2–5.5) within vesicles,[17,18] required for the transport of neurotransmitters into the vesicle lumen. In addition to the established role of vH^+-ATPase in neurotransmitter transport into SVs, vH^+-ATPase has been suggested to participate in the secretion of stored neurotransmitters.[19,20] Furthermore, guanine nucleosides have been reported to influence the glutamate-induced cellular response via diverse trophic, proliferative and modulatory effects of the nucleotide on neurons.[21] Since SV swelling is $G_{\alpha o}$ mediated and is required for cell secretion,[10] it could be hypothesized that the vH^+-ATPase in SV membrane[15,16] may participate in $G_{\alpha o}$-mediated water gating through the AQP-6 channels at the vesicle membrane, resulting in vesicle swelling. This hypothesis was tested in a recent study,[22] and, in agreement, results from the study demonstrate that the SV-associated vH^+-ATPase is required for GTP-$G_{\alpha o}$-mediated swelling of vesicles. In view of this, the involvement of cholesterol in SV swelling was hypothesized and tested in the current study using isolated SVs and the determination of their swelling competency in the presence and absence of cholesterol. Depletion of cholesterol from SV membrane was found to result in a significant loss of GTP-mastoparan-stimulable swelling. In contrast, addition of cholesterol to isolated SVs potentiates GTP-mastoparan-stimulable vesicle swelling. Our study further demonstrates that this cholesterol effect is, in part, due to its influence in regulating the interactions between AQP-6, vH^+-ATPase and the GTP-binding $G_{\alpha o}$ protein at the SV membrane.

Materials and methods

Synaptosome and SV isolation

Synaptosomes and SVs were prepared from rat brains using published procedures.[10,14] Whole brain from Sprague–Dawley rats, weighing 100–150 g, was isolated and placed in ice-cold-buffered sucrose solution (5 mmol/L Hepes [4-(2-hydroxyethyl)-1-piperazineethanesulfonic acid], pH 7.4, 0.32 mmol/L sucrose), supplemented with protease inhibitor cocktail (Sigma, St Louis, MO, USA). The brain tissue was homogenized using 8–10 strokes in a Teflon-glass homogenizer. The total homogenate was centrifuged for three minutes at 2500 *g* and the supernatant fraction was further centrifuged for 15 min at 14,500 *g* to obtain a pellet. The resultant pellet was resuspended in buffered sucrose solution and loaded onto a 3–10–23% Percoll gradient. After centrifugation at 28,000 *g* for six minutes, the enriched synaptosome fraction was collected at the 10–23% Percoll gradient interface. To isolate SVs, the synaptosome preparation was diluted using 9 vol of ice-cold water, followed by 30 min incubation on ice, resulting in the lysis of synaptosomes to release SVs. The homogenate was then centrifuged for 20 min at 25,500 *g* and the resultant supernatant enriched in SVs was obtained.

Measurement of SV size

The measurement of SV size was carried out using photon correlation spectroscopy (PCS) and right-angle light scattering. Changes in SV size were determined using PCS. PCS is a well-known technique for the measurement of the size of micrometer- to nanometer-sized particles and macromolecules. PCS measurements were performed in a Zetasizer Nano ZS (Malvern Instruments, Worcestershire, UK). In a typical experiment, the size distribution of isolated SVs was determined using built-in software provided by Malvern Instruments. Prior to determination of the vesicle hydrodynamic radius, calibration of the instrument was performed using latex spheres of known size. In PCS, subtle fluctuations in the sample scattering intensity are correlated across microsecond timescales. The correlation function was calculated, from which the diffusion coefficient was determined. Using the Stokes–Einstein equation, the hydrodynamics radius can be acquired from the diffusion coefficient.[23] The intensity size distribution, which is obtained as a plot of the relative intensity of light scattered by particles in various size classes, is then calculated from a correlation function using built-in software. The particle scattering intensity is proportional to the molecular weight squared. Volume distribution can be derived from the intensity distribution using Mie theory.[24,25] The transforms of the PCS intensity distribution to volume distributions can be obtained using the software provided by Malvern Instruments. In experiments, isolated SVs were suspended in isotonic buffer containing 0.3 mmol/L sucrose, 10 mmol/L Hepes (pH 7.4) and 20 mmol/L KCl, and changes in vesicle size were monitored before and after the addition of 20 μmol/L GTP-20 μmol/L mastoparan and/or 10, 20 and 40 μmol/L methyl β-cyclodextrin (MβCD) (Sigma, St Louis, MO, USA). Student's *t*-test was performed for comparison between groups ($n = 5$) with significance established at $P < 0.05$(*). Similarly, the measurement of SV size dynamics was determined using realtime, right-angle light scattering in a Hitachi F-2000 spectrofluorometer. Realtime scattered light intensities at 600 nm were measured as a function of vesicle radius.[26] Changes in vesicle size were monitored before and after the addition of 20 μmol/L GTP-20 μmol/L mastoparan and/or 20 μmol/L and 40 μmol/L MβCD (Sigma). Values are expressed in arbitrary units and as percent light scattered over controls. Student's *t*-test was performed for comparison between groups with significance established at $P < 0.05$(*).

Immunoblot analysis and immunoisolation

Protein content in the various brain fractions were determined by the bicinchoninic acid (BCA) assay (Pierce BCA protein Assay Kit, Pierce Biotechnology, Rockford, IL, USA). Sample aliquots solubilized in Laemmli sample preparation buffer were resolved using 10% sodium dodecyl sulfate-polyacrylamide gel electrophoresis (SDS-PAGE). Five micrograms of protein, each from total brain

homogenate (BH), synaptosomes (SS) and SV fractions, were resolved using SDS-PAGE and electrotransferred to 0.2-mm-thick nitrocellulose membranes for immunoblot analysis using specific antibodies to vesicle-associated membrane protein 2 (VAMP-2; Sigma) and AQP-6 (Santa Cruz, CA, USA) for immunoblot analysis. Similarly, 5 μg SV protein/lane was resolved using the SDS-PAGE, followed by electrotransfer to nitrocellulose membranes for immunoblot analysis using specific antibodies to VAMP-2, AQP-6, vH^+-ATPase and $G_{\alpha o}$ (Santa Cruz). The nitrocellulose membranes were incubated for one hour at 4°C in blocking buffer (5% non-fat milk in phosphate-buffered saline (PBS) containing 0.1% Triton X-100 and 0.02% NaN_3) and immunoblotted for one hour at room temperature with the primary antibody. The immunoblotted nitrocellulose membranes were washed (3×) in PBS containing 0.1% Triton X-100 and 0.02% NaN_3, and incubated for one hour at room temperature in horseradish peroxidase-conjugated secondary antibody at a dilution of 1:1000 in blocking buffer. The immunoblots were then washed (3×) in PBS, processed for enhanced chemiluminescence and photographed using a Kodak Image Station 414.

Immunoisolation studies were performed using 100 μg of Triton/Lubrol- and Triton/Lubrol–Saponin-solubilized SV protein to determine the role of cholesterol on the physical interaction between AQP-6, $G_{\alpha o}$ and vH^+-ATPase at the SV. One hundred micrograms of SV homogenate were prepared by solubilizing SVs in Triton/Lubrol solubilization buffer (1% Lubrol; 1 mmol/L benzamidine; 5 mmol/L Mg-ATP; 5 mmol/L ethylenediaminetetraacetic acid; 1% Triton X-100, in PBS) in the absence and presence of saponin (1% [w/v]) supplemented with protease inhibitor cocktail (Sigma). AQP-6 or $G_{\alpha o}$ antibody conjugated to A/G Plus-Agarose beads (Santa Cruz) were incubated with the solubilized SV preparation for one hour at room temperature, followed by washing with PBS. The immunoisolated samples bound to the immuno-sepharose beads were eluted using low pH buffer and subsequently brought to neutral pH. SDS-PAGE, electrotransfer to nitrocellulose, followed by immunoblot analysis, were then performed on the immunoisolated material. AQP-6 immunoisolates were probed with $G_{\alpha o}$- and vH^+-ATPase-specific antibody, and the $G_{\alpha o}$ immunoisolate was probed with vH^+-ATPase-specific antibody to determine the physical interaction between these proteins at the SV.

Resolving $G_{\alpha o}$-associated complexes in solubilized SV membrane fractions using continuous sucrose density gradient centrifugation

Freshly isolated SVs were solubilized in ice-cold Triton/Lubrol (1% [w/v]) PBS in the absence or presence of saponin (1% [w/v]) supplemented with protease inhibitor cocktail. Total solubilized protein (0.35 mg) in a volume of 200 μL was loaded onto a linear 10–50% sucrose density gradient and centrifuged at 300,000 g at 4 °C for three hours in a Beckman TLA 100.3 bench-top ultracentrifuge. A total of 13 fractions were collected from the top and analyzed for the presence of the $G_{\alpha o}$ protein, using immunoblot analysis.

Atomic force microscopy

Isolated SVs in the buffer were plated on freshly cleaved mica, to be imaged using the atomic force microscope (AFM). Ten minutes after plating, the mica disk was placed in a fluid chamber and washed with the incubation buffer to remove unattached SV, prior to imaging in the presence or absence of 20 μmol/L GTP-20 μmol/L mastoparan and/or 10, 20 and 40 μmol/L MβCD (Sigma), or 20 μmol/L cholesterol. Isolated SVs were imaged using the Nanoscope IIIa, Digital Instruments (Santa Barbara, CA, USA). All images presented in this study were obtained in the 'tapping' mode in fluid, using silicon nitride tips with a spring constant of 0.06 N m^{-1} and an imaging force of less than 200 pN. Images were obtained at line frequencies of 2.523 Hz, with 512 lines per image and constant image gains. Topographical dimensions of SV were analyzed using the NANOSCOPE (R) IIIA 4.43r8 software, supplied by Digital Instruments.

Results and discussion

In contrast to slow water entry by diffusion, GTP-mastoparan induces the rapid swelling of SVs via facilitated transport of water molecules through water channels or AQPs at the SV membrane.[14] In these earlier studies,[14] AQP-6 at the SV membrane was demonstrated to be involved in GTP-mastoparan-induced SV swelling.[14] Results from a recent study[22] further demonstrate that the G_{ao}-stimulated SV swelling is vH^+-ATPase dependent and pH sensitive. Since water channels including AQP-6 are bi-directional, and the vH^+-ATPase inhibitor bafilomycin decreases the volume of resting SVs, this suggests that vH^+-ATPase is upstream of AQP-6, in the pathway leading from G_{ao}-stimulated swelling of SVs. Vesicle acidification is therefore a prerequisite for AQP-6-mediated rapid gating of water into SVs. This was the first direct demonstration of the involvement of SV membrane-associated vH^+-ATPase in G_{ao}-stimulated swelling.

In the current study, AFM of isolated synaptosomes (Figure 1a) and SVs (Figure 1b and c), and immunoblot analysis (Figure 1d) demonstrate a highly enriched SV preparation. SVs were found to have a mean diameter of 45 nm. Immunoblot analysis further demonstrated the SV preparation to be enriched in VAMP-2 and AQP-6 (Figure 1d), both SV-specific proteins.[14] Collectively, these studies demonstrate the isolation of a highly enriched SV preparation from rat brain tissue for our SV swelling assays.

To determine the role of cholesterol on GTP-mastoparan-stimulable SV swelling, the size of isolated SV was monitored before and after exposure to MβCD. Both β-cyclodextrin and MβCD remove cholesterol from cellular membrane. MβCD is more efficient than β-cyclodextrin and is water-soluble. MβCD is known to form soluble inclusion complexes with cholesterol, thereby enhancing its solubility in aqueous solution. Our studies using both dynamic light scattering (DLS) (Figure 2a) and PCS (Figure 2b) demonstrate an MβCD dose-dependent inhibition of GTP-mastoparan-stimulable SV swelling. To further determine the role of cholesterol on GTP-mastoparan-stimulable SV

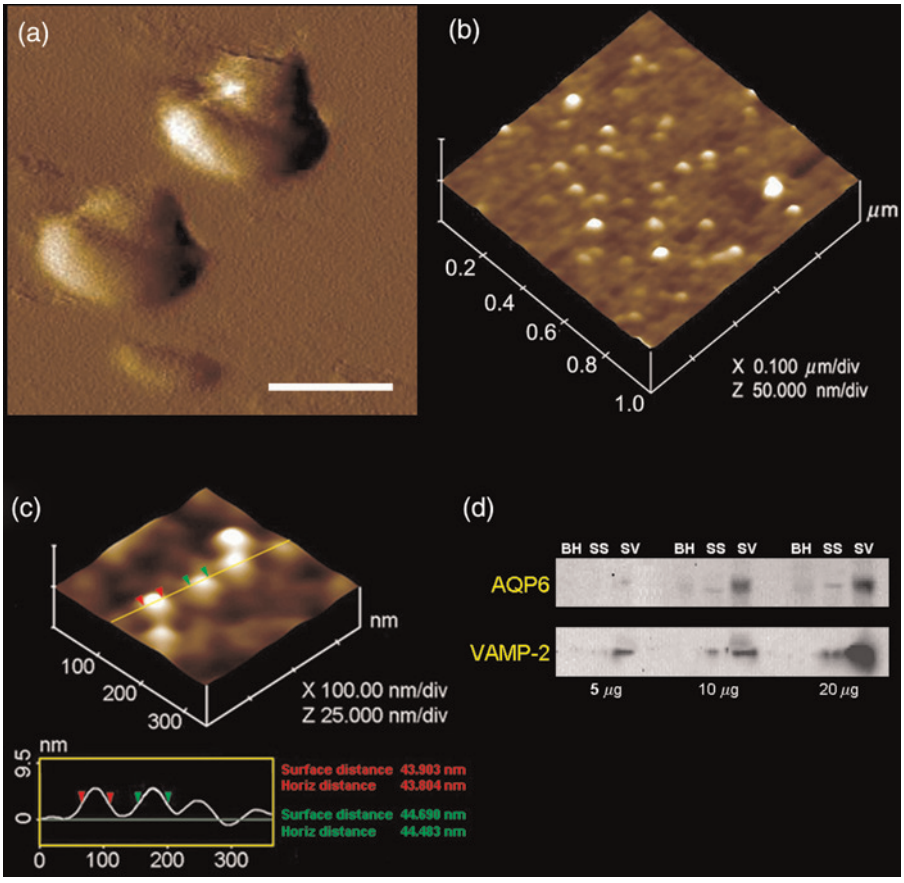

Figure 1 Atomic force micrographs of isolated synaptosomes and synaptic vesicles. Purity of isolated synaptosomes (SS) (a) (bar = 1 μm) and synaptic vesicle (SV) (b and c) preparation were determined using atomic force microscopy (AFM) (a–c) and immunoblot analysis (d). Note the mushroom-shaped synaptosomes in the atomic force micrograph (a). Atomic force micrographs demonstrate the average size of SVs to be approximately 45 nm. Note the AFM section analysis of two SVs. Immunoblot analysis of 5, 10 and 20 μg protein each, of total rat brain homogenate (BH), SS and SVs, demonstrates the enriched presence of SV proteins, vesicle-associated membrane protein-2 (VAMP-2) and the water channel AQP-6 in the SV fraction (A color version of this figure is available in the online journal)

swelling, the size and relative volume of isolated SV was monitored before and after exposure to MβCD and cholesterol, using the AFM (Figure 3). In agreement with our findings using DLS and PCS, our AFM studies demonstrate an MβCD dose-dependent inhibition of GTP-mastoparan-stimulable SV swelling. Additionally, the exposure of SV to 20 μmol/L cholesterol demonstrates a significant increase in GTP-mastoparan-stimulable SV swelling (Figure 3). Collectively, these studies using DLS, PCS and AFM clearly demonstrate that cholesterol at the SV membrane is critical in the regulation of SV volume. Since the GTP-binding proteins $G_{\alpha o}$, AQP-6[14] and vH^+-ATPase[22] have been implicated in SV swelling, and depletion of cholesterol affects SV swelling, the influence of cholesterol on the interaction between these proteins at the SV membrane was investigated.

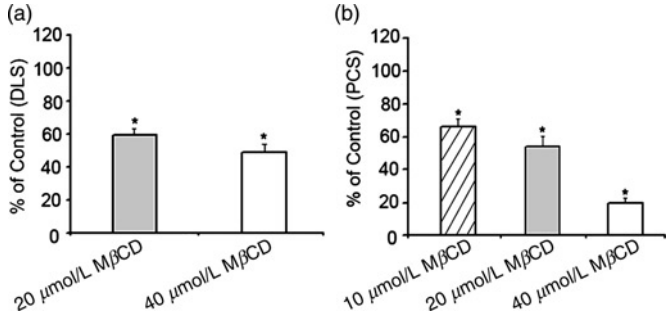

Figure 2 Guanosine triphosphate-mastoparan (Mas)-induced synaptic vesicle (SV) swelling is cholesterol sensitive. Isolated SVs swell in response to 20 μmol/L GTP-20 μmol/L Mas (GTP-Mas w/o methyl β-cyclodextrin [MβCD]), as demonstrated using dynamic light scattering (DLS) (a) and photon correlation spectroscopy (PCS) (b). Note the MβCD dose-dependent inhibition of GTP-Mas-stimulable SV swelling, demonstrated by both DLS and PCS measurements. Student's *t*-test was performed for comparison between groups ($n = 4$) with significance established at $P < 0.05$(*)

To confirm the presence of VAMP-2, AQP-6, vH^+-ATPase and $G_{\alpha o}$ in our SV preparation, 5 μg SV protein/lane was resolved using SDS-PAGE, followed by electrotransfer to nitrocellulose membranes for immunoblot analysis using specific antibodies to VAMP-2, AQP-6, vH^+-ATPase and $G_{\alpha o}$. Results from these studies demonstrate the presence of VAMP-2, AQP-6, vH^+-ATPase and $G_{\alpha o}$ in the SV fraction (Figure 4a). To determine the role of cholesterol on the physical interaction between AQP-6, $G_{\alpha o}$ and vH^+-ATPase at the SV, further immunoisolation studies were performed using 100 μg of Triton/Lubrol- and Triton/Lubrol–Saponin-solubilized SV protein (Figure 4b). Immunoisolation of Triton/Lubrol-solubilized SV protein using AQP-6 antibody

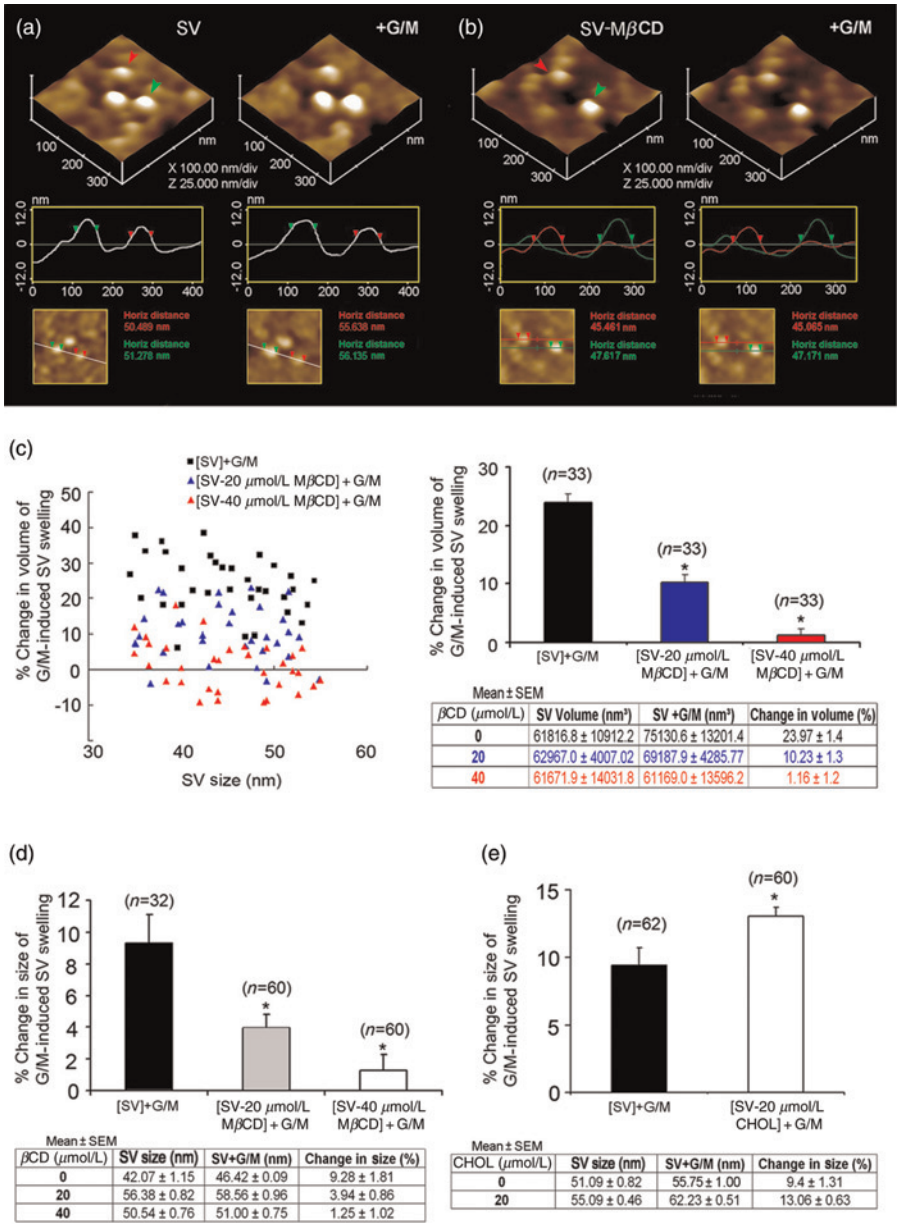

Figure 3 Atomic force micrographs of synaptic vesicles (SVs) demonstrating methyl β-cyclodextrin (MβCD) dose-dependent inhibition of GTP-mastoparan-induced swelling. In conformation with photon correlation spectroscopy and dynamic light scattering studies (Figure 2), isolated SVs (a, left) swell when exposed to 20 μmol/L GTP-20 μmol/L mastoparan (G/M) (a, right). Exposure of SVs to 40 μmol/L MβCD significantly inhibits G/M-induced vesicle swelling (b, right). Note the MβCD dose-dependent loss in G/M-induced SV volume (c, $n = 33$, $^*P < 0.05$) and diameter (d, control $n = 32$, 20 μmol/L MβCD $n = 60$, 40 μmol/L MβCD $n = 60$, $^*P < 0.05$). SVs of size distribution 35–55 nm all respond similarly to MβCD (c, left panel). Exposure of SVs to 20 μmol/L cholesterol (CHOL) $n = 60$ demonstrates a significant increase in G/M-induced swelling (e, $n = 60$). Raw data for c–e are presented in the tables immediately below the bar graphs (A color version of this figure is available in the online journal)

demonstrates the co-isolation of both $G_{\alpha o}$ and vH^+-ATPase. Similarly, immunoisolation of Triton/Lubrol-solubilized SV protein using $G_{\alpha o}$ antibody demonstrates the co-isolation of the vH^+-ATPase protein. Saponin has the ability to partition cholesterol from membrane proteins. When the Triton/Lubrol/Saponin-solubilized SV preparation was used to immunoisolate AQP-6- and $G_{\alpha o}$-associated proteins, a significant loss in their interactions is demonstrated. To further confirm the role of cholesterol on the interaction between the above proteins, Triton/Lubrol- and Triton/Lubrol–Saponin-solubilized SV fractions were resolved using a continuous sucrose density gradient. Larger complexes would tend to migrate toward the bottom of the gradient, and the lighter ones at the upper end. In conformation, immunoblot analysis of equal volume of the Triton/Lubrol-solubilized SV fractions using $G_{\alpha o}$ antibody demonstrates a larger complex at the bottom of the gradient (Figure 4c). In contrast, the Triton/Lubrol–Saponin-solubilized SV fraction shows the $G_{\alpha o}$-specific immunoreactivity to be at the upper end of the gradient (Figure 4c), demonstrating disassembly of the $G_{\alpha o}$-associated complex.

Secretory vesicle swelling is required for cell secretion.[10] In the current study, utilizing a number of approaches to determine nanometer-scale changes in SV size, the role of

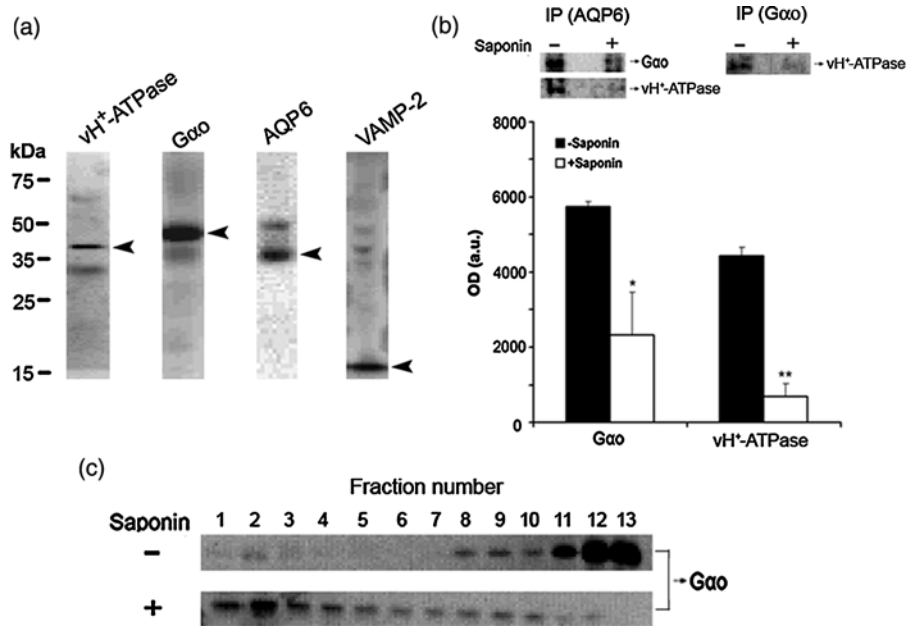

Figure 4 Depletion of cholesterol from synaptic vesicle (SV) results in the loss of interactions between aquaporin-6 (AQP-6), vH^+-ATPase and the GTP-binding $G_{\alpha o}$ proteins at the SV. (a) Immunoblot analysis of 5 μg SV protein lane, demonstrating the presence of vH^+-ATPase-, $G_{\alpha o}$-, AQP-6- and vesicle-associated membrane protein-(VAMP)2-specific immunoreactivity. (b) Immunoisolation of 100 μg of Triton/Lubrol-solubilized SV protein using AQP-6 antibody, demonstrating the co-isolation of both $G_{\alpha o}$ and vH^+-ATPase proteins. Similarly, immunoisolation of the same amount of Triton/Lubrol-solubilized SV protein using $G_{\alpha o}$ antibody, demonstrating the co-isolation of the vH^+-ATPase protein. On the contrary, when Triton/Lubrol/Saponin-solubilized SV preparation was used to immunoisolate AQP-6- and $G_{\alpha o}$-associated proteins, a significant loss in their interactions is observed. (c) Immunoblot analysis of an equal volume of Triton/Lubrol-solubilized SV fractions using $G_{\alpha o}$ antibody demonstrating a larger $G_{\alpha o}$-specific complex at the bottom of the gradient. In contrast, the Triton/Lubrol–Saponin-solubilized SV fraction shows the $G_{\alpha o}$-specific immunoreactivity to be at the upper end of the gradient (c), demonstrating disassembly of the $G_{\alpha o}$-associated complex in the absence of cholesterol

cholesterol in the regulation of SV volume was determined. Unlike slow water entry by diffusion, GTP-mastoparan induces a rapid swelling of SVs via facilitated transport of water molecules through the water channel or AQP-6 at the SV membrane.[14] AQP-6 at the SV membrane is demonstrated to be involved in GTP-mastoparan-induced SV swelling.[14] The earlier demonstration[22] that $G_{\alpha o}$-stimulated SV swelling is vH^+-ATPase dependent, and the influence of cholesterol on neurotransmitter release,[2,3] prompted the current study to determine the role of cholesterol in the SV volume regulation. The depletion of cholesterol from SV results in a significant loss of GTP-mastoparan-stimulable SV swelling. In contrast, the addition of cholesterol to the SV preparation potentiates GTP-mastoparan-stimulable vesicle swelling. Our study further demonstrates that cholesterol is required for the interactions between AQP-6, vH^+-ATPase and the GTP-binding $G_{\alpha o}$ protein at the SV.

The overall physiological relevance of vesicle swelling, and the role of cholesterol in neurotransmitter release, has become clear. As briefly outlined in the introduction, vesicle volume increase following stimulation of cell secretion is critical in the expulsion of intravesicular contents.[10] In earlier studies,[10] isolated live pancreatic acinar cells in near physiological buffer when imaged using an AFM at high force (200–300 pN) demonstrate the size and shape of the secretory vesicles (ZGs) lying immediately below the apical plasma membrane of the cell. Within 2.5 min of exposure to a physiological secretory stimulus, the majority of ZGs within cells swell, followed by a decrease in ZG size following secretion. These studies revealed for the first time, in live cells, intracellular swelling of secretory vesicles following stimulation of secretion, and their deflation following partial discharge of vesicular contents.[10] No loss of secretory vesicles is observed throughout the experiment. Similarly, isolated synaptosomal membrane when placed on mica and imaged by an AFM in near physiological buffer reveals, on the cytosolic compartment, the presence of 40–50 nm diameter SVs, still docked to the presynaptic membrane. As with ZGs, exposure of SVs to 20 μmol/L GTP results in SVs swelling, and a decrease following exposure to Ca^{2+}, resulting from the transient fusion of SVs at the presynaptic membrane and neurotransmitter release.[10] Additionally, as observed in ZGs, not all SVs swell, and if they did, they swell to different extents even though they have been exposed to the same stimulus. This differential response of SVs within the same nerve ending may dictate and regulate the potency and efficacy of neurotransmitter release at the nerve terminal.[10] The role of vesicle swelling in cell secretion has been further documented using electrophysiological bilayer fusion assays. Functionally reconstituted porosomes (the universal secretory machinery at the cell plasma membrane), at the lipid membrane of a bilayer apparatus, where membrane conductance and capacitance can be continually monitored, have been used.[10] Isolated ZGs, when added to the *cis* compartment of the bilayer chamber, fuse at the porosome-reconstituted lipid membrane, and are detected as a step increase in membrane capacitance. Results from these experiments demonstrate that even after 15 min of ZG

addition to the *cis* compartment of the bilayer chamber, little or no release of the intravesicular enzyme α-amylase is detected in the trans-compartment. On the contrary, exposure of ZGs to 20 mmol/L GTP promotes swelling[11–14] and results in a robust expulsion of α-amylase into the trans-compartment of the bilayer chamber. These studies demonstrate that during secretion, secretory vesicle swelling is required for the expulsion of intravesicular contents. This mechanism of vesicular expulsion during cell secretion explains why partially empty vesicles are observed in the electron micrographs of cells[9,27] following secretion. In agreement, it has been demonstrated that 'secretory granules are recaptured largely intact after stimulated exocytosis in cultured endocrine cells',[28] that 'single SVs fuse transiently and successively without loss of identity'[29] and that 'ZG exocytosis is characterized by long fusion pore openings and preservation of vesicle lipid identity'.[30]

Membrane cholesterol has been widely viewed as a molecule responsible in the establishment of membrane domains, and in influencing membrane curvature. We now know that cholesterol has a much wider dynamic function, such as its direct interaction and influence on membrane proteins and their function, on protein–protein interactions and the like. In neurons, cholesterol is found to be a prominent molecule of SV membranes[31] and has been suggested to function as a spatial organizer of SV and its recycling.[32] Therefore, it is no surprise that cholesterol is involved in SV biogenesis,[33] and defects in cholesterol homoeostasis in the brain have been linked to the development of several neurological disorders, including Alzheimer's disease and Niemann–Pick type C disease.[34] Recent studies on the neuronal porosome complex[35] demonstrate the critical role of cholesterol in its structural integrity. Results from the study demonstrate a significant inhibition in interactions between porosome-associated t-SNAREs (target-membrane-associated-soluble *N*-ethylmaleimide fusion protein attachment protein receptor) and calcium channels following depletion of membrane cholesterol. Since calcium is critical to SNARE-induced membrane fusion,[36–38] the loss of interaction between SNAP-25, Syntaxin-1 and the calcium channel at the neuronal porosome complex would seriously compromise or abrogate neurotransmission at the nerve terminal.

Author contributions: J-SL performed most of the SV isolation and characterization and the biochemical, dynamic light scattering and PCS experiments. WJC performed the atomic force microscopy studies, and LS helped in SV preparation and in some of the PCS studies. BPJ helped in the development and design of experiments and in part writing of the manuscript.

ACKNOWLEDGEMENTS

This work was supported by NIH Grant NS39918 and by the Wayne State University Research Enhancement Award (BPJ).

REFERENCES

1 Mukherjee S, Maxfield FR. Membrane domains. *Annu Rev Cell Dev Biol* 2004;**20**:839–66
2 Zamir O, Charlton MP. Cholesterol and synaptic transmitter release at crayfish neuromuscular junctions. *J Physiol* 2006;**571**:83–99
3 Cho WJ, Jeremic A, Jin H, Ren G, Jena BP. Neuronal fusion pore assembly requires membrane cholesterol. *Cell Biol Int* 2007;**31**:1301–8
4 Koudinov AR, Koudinova NV. Essential role for cholesterol in synaptic plasticity and neuronal degeneration. *FASEB J* 2001;**15**:1858–60
5 Fernandez JM, Villalón M, Verdugo P. Reversible condensation of mast cell secretory products *in vitro*. *Biophys J* 1991;**59**:1022–7
6 Curran MJ, Brodwick MS. Ionic control of the size of the vesicle matrix of beige mouse mast cells. *J Gen Physiol* 1991;**98**:771–90
7 Monck JR, Oberhauser AF, Alvarez de Toledo G, Fernandez JM. Is swelling of the secretory granule matrix the force that dilates the exocytotic fusion pore? *Biophys J* 1991;**59**:39–47
8 Alvarez de Toledo G, Fernández-Chacón R, Fernández JM. Release of secretory products during transient vesicle fusion. *Nature* 1993;**363**:554–8
9 Cho S-J, Cho J, Jena BP. The number of secretory vesicles remains unchanged flowing exocytosis. *Cell Biol Int* 2002;**26**:29–33
10 Kelly M, Cho WJ, Jeremic A, Abu-Hamdah R, Jena BP. Vesicle swelling regulates content expulsion during secretion. *Cell Biol Int* 2004;**28**:709–16
11 Cho S-J, Sattar AK, Jeong EH, Satachi M, Cho HA, Dash S, Mayes MS, Stromer MH, Jena BP. Aquaporin 1 regulates GTP-induced rapid gating of water in secretory vesicles. *Proc Natl Acad Sci USA* 2002;**99**:4720–4
12 Jena BP, Schneider SW, Geibel JP, Webster P, Oberleithner H. G_i regulation of secretory vesicle swelling examined by atomic force microscopy. *Proc Natl Acad Sci USA* 1997;**94**:13317–22
13 Abu-Hamdah R, Cho WJ, Cho SJ, Jeremic A, Kelly M, Llie AE, Jena BP. 'Regulation of the water channel aquaporin-1' isolation and reconstitution of the regulatory complex. *Cell Biol Int* 2004;**28**:7–17
14 Jeremic A, Cho WJ, Jena BP. Involvement of water channels in synaptic vesicle swelling. *Exp Biol Med* 2005;**230**:674–80
15 Stadler H, Tsukita S. Synaptic vesicles contain an ATP-dependent proton pump and show 'knob-like' protrusions on their surface. *EMBO J* 1984;**3**:3333–7
16 Hicks B, Parsons S. Characterization of the P-type and V-type ATPases of cholinergic synaptic vesicles and coupling of nucleotide hydrolysis to acetylcholine transport. *J Neurochem* 1992;**58**:1211–20
17 Michaelson D, Angel I. Determination of ΔpH in cholinergic synaptic vesicles: its effect on storage and release of acetylcholine. *Life Sci* 1980;**27**:39–44
18 Füldner H, Stadler H. ^{31}P-NMR analysis of synaptic vesicles. Status of ATP and internal pH. *Eur J Biochem* 1982;**121**:519–24
19 Morel N, Dunant Y, Israël M. Neurotransmitter release through the V0 sector of V-ATPase. *J Neurochem* 2001;**79**:485–8
20 Peters C, Bayer M, Bühler S, Andersen J, Mann M, Mayer A. Trans-complex formation by proteolipid channels in the terminal phase of membrane fusion. *Nature* 2001;**409**:581–8
21 Santos T, Souza D, Tasca C. GTP uptake into rat synaptic vesicles. *Brain Res* 2005;**1070**:71–6
22 Shin L, Basi N, Lee J-S, Cho WJ, Chen Z, Abu-Hamdah R, Oupicky D, Jena BP. Involvement of vH^+-ATPase in synaptic vesicle swelling. *J Neurosci Res* 2010;**88**:95–101
23 Higashijima T, Uzu S, Nakajima T, Ross E. Mastoparan, a peptide toxin from wasp venom, mimics receptors by activating GTP-binding regulatory proteins (G proteins). *J Biol Chem* 1988;**263**:6491–4
24 Vitale N, Mukai H, Rouot B, Thierse D, Aunis D, Bader MF. Exocytosis in chromaffin cells. Possible involvement of the heterotrimeric GTP-binding protein G(o). *J Biol Chem* 1993;**268**:14715–23
25 Weingarten R, Ransnas L, Mueller H, Sklar L, Bokoch G. Mastoparan interacts with the carboxyl terminus of the alpha subunit of Gi. *J Biol Chem* 1990;**265**:11044–9
26 Matsuzaki K, Murase O, Sugishita K, Yoneyama S, Akada K, Ueaha M, Nakamura A, Kobayashi S. Optical characterization of liposomes by right angle light scattering and turbidity measurements. *Biochem Biophys Acta* 2000;**1467**:219–26
27 Lawson D, Fewtrell C, Gomperts B, Raff M. Anti-immunoglobulin-induced histamine secretion by rat peritoneal mast cells studied by immunoferritin electron microscopy. *J Exp Med* 1975;**142**:391–401

28 Taraska JW, Perrais D, Ohara-Imaizumi M, Nagamatsu S, Almers W. Secretory granules are recaptured largely intact after stimulated exocytosis in cultured endocrine cells. *Proc Natl Acad Sci USA* 2003;**100**:2070–5
29 Aravanis AM, Pyle JL, Tsien RW. Single synaptic vesicles fusing transiently and successively without loss of identity. *Nature* 2003;**423**:643–7
30 Thorn P, Fogarty KE, Parker I. Zymogen granule exocytosis is characterized by long fusion pore openings and preservation of vesicle lipid identity. *Proc Natl Acad Sci USA* 2004;**101**:6774–9
31 Deutsch JW, Kelly RB. Lipids of synaptic vesicles: relevance to the mechanism of membrane fusion. *Biochemistry* 1981;**20**:378–85
32 Jia J-Y, Lamer S, Schuemann M, Schmidt MR, Krause E, Haucke V. Quantitative proteomic analysis of detergent-resistant membranes from chemical synapses: evidence for cholesterol as spatial organizer of synaptic vesicle cycling. *Mol Cell Proteomics* 2006;**5**:2060–71
33 Thiele C, Hannah MJ, Fahrenholz F, Huttner WB. Cholesterol binds to synaptophysin and is required for biogenesis of synaptic vesicles. *Nat Cell Biol* 2000;**2**:42–9
34 Vance JE, Karten B, Hayashi H. Lipid dynamics in neurons. *Biochem Soc Trans* 2006;**34**:399–403
35 Cho WJ, Jeremic A, Jin H, Ren G, Jena BP. Neuronal fusion pore assembly requires membrane cholesterol. *Cell Biol Int* 2007;**31**:1301–8
36 Cho WJ, Jeremic A, Jena BP. Direct interaction between SNAP-23 and L-type calcium channel. *J Cell Mol Med* 2005;**9**:380–6
37 Jeremic A, Kelly M, Cho J, Cho S, -J JK, Jena BP. Calcium drives fusion of SNARE-apposed bilayers. *Cell Biol Int* 2004a;**28**:19–31
38 Jeremic A, Cho WJ, Jena BP. Membrane fusion: what may transpire at the atomic level. *J Biol Phys Chem* 2004;**4**:139–42

(Received August 25, 2009, Accepted January 8, 2010)